

Dipolar and Quadrupolar Freezing in $(\text{KBr})_{1-x}(\text{KCN})_x$

U. G. Volkman, R. Böhmer, A. Loidl, and K. Knorr

Institut für Physik, Universität Mainz, D-6500 Mainz, Federal Republic of Germany

U. T. Höchli

IBM Zürich Research Laboratories, CH-8803 Rüschlikon, Switzerland

and

S. Haussühl

Institut für Kristallographie, Universität zu Köln, D-5000 Köln, Federal Republic of Germany

(Received 20 September 1985)

Dipolar and quadrupolar susceptibility measurements are reported for the molecular glass system $(\text{KBr})_{1-x}(\text{KCN})_x$ covering a wide range of frequencies. The results allow a direct comparison of the dipolar and quadrupolar anomalies and demonstrate unambiguously that the freezing in of the dipolar and quadrupolar degrees of freedom occurs at different temperatures.

PACS numbers: 61.40.+b, 62.20.Dc, 77.20.+y

The mixed molecular crystals $(\text{KBr})_{1-x}(\text{KCN})_x$ show a fascinating (x, T) phase diagram.¹ The room-temperature structure is NaCl-type with the CN molecules being rotationally disordered. In this high-temperature plastic phase each CN^- ion undergoes fast reorientations. For $x \geq 0.6$ four crystallographic low-temperature phases have been reported,^{1,2} where the orientational degrees of freedom are reduced. Only in the orthorhombic phases ($0.9 \leq x \leq 1$, $T \leq 80$ K) is the orientational order complete.² All the other phases exhibit dipolar disorder characterized by a residual degeneracy with respect to head and tail down to the lowest temperatures. Crystals with $x \leq 0.6$ remain in a quadrupolar disordered state of quasicubic structure with frozen-in random CN orientations and frozen-in lattice strains.^{3,4} Recently, tremendous experimental and theoretical efforts have been undertaken to investigate the possibility of a molecular glass state⁵⁻¹⁸ in this concentration region.

So far, slowing down of the reorientational motion of the CN^- ions has been described in terms of dielectric dispersion at frequencies $\nu < 1$ MHz and in terms of elastic dispersion for $\nu > 1$ MHz. Although these data have been described by a unique Arrhenius law,^{6,10} the question remained open whether both dispersion regimes belong to the same relaxation mechanism. In this Letter we will present data on the elastic and dielectric dispersion which cover a common frequency range $10^2 \text{ Hz} < \nu < 10^9 \text{ Hz}$ and allow a direct comparison of the quadrupolar and the dipolar anomalies. In particular, it will be demonstrated that the freezing in of dipoles and quadrupoles occurs at different temperatures.

The temperature dependence of the elastic constant c_{44} has been determined by a torsion pendulum with eigenfrequencies ν ranging from 50 Hz to 1 kHz using capacitive drive and pickup.¹⁹ The pendulum consists of a single crystal as active element with a typical size

of $2 \times 2 \times 6 \text{ mm}^3$ and the capacitor plates acting as a moment of inertia.¹⁹ The torque is parallel to [100]. Data for $c_{44}(T, \nu)$ for a crystal with a concentration of $x = 0.2$ are shown in Fig. 1. In addition ultrasonic,⁸ Brillouin,²⁰ and inelastic-neutron-scattering⁹ results are indicated in Fig. 1. $c_{44}(T, \nu)$ softens, passes through a minimum, and recovers again towards 0 K. $c_{44}(T, \nu)$ is related to the quadrupolar susceptibility of the orientational subsystem $\chi^Q(T, \nu)$ via

$$c_{44}(T, \nu) = c_{44}^0 [1 - g^2 \chi^Q(T, \nu)],$$

where ν is the measuring frequency, c_{44}^0 is the background elastic constant, and g is the rotation-translation coupling coefficient.³ From Fig. 1 one notes frequency-dependent cusps of the quadrupolar susceptibility.

Measurements of the dielectric constant $\epsilon(T, \nu)$

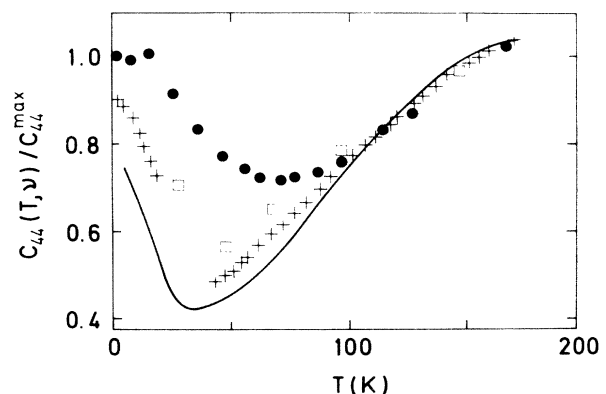


FIG. 1. Normalized elastic constant c_{44} vs temperature as determined in $(\text{KBr})_{0.8}(\text{KCN})_{0.2}$ for different measuring frequencies: terahertz, inelastic-neutron-scattering studies (Ref. 9) (full circles); gigahertz, Brillouin data ($x = 0.19$) (Ref. 20) (open squares); 10 MHz, ultrasonic results (Ref. 8) (plusses); kilohertz, torsion pendulum measurements (solid line).

probe the dipolar susceptibility $\chi^D(T, \nu)$: $\epsilon(T, \nu) = \epsilon_\infty + 4\pi\chi^D(T, \nu)$. The results of the real part of $\epsilon(T, \nu)$ in $(\text{KBr})_{0.8}(\text{KCN})_{0.2}$ are shown in Fig. 2. The low-frequency data are taken from Ref. 11. The high-frequency data have been obtained by measurement of reflection coefficient and phase shift utilizing an automatic rf impedance analyzer.

Both dipolar and quadrupolar susceptibilities χ^D and χ^Q are given by $\chi^{D,Q}(T, \nu) \propto 1/k_B T [1 + i\omega\tau^{D,Q}(T)]$. Here $\omega = 2\pi\nu$, and τ^D is the dipolar and τ^Q the quadrupolar relaxation time. As the temperature is lowered the molecular relaxation slows down yielding dispersion in the real part and a loss peak in the imaginary part of the orientational susceptibility. The maximum in the loss appears as $\omega\tau = 1$ defining the temperature where the relaxation rates equal a given measuring frequency. As no quadrupolar loss data are available,²¹ we took the maxima of the real parts of the susceptibilities defined by $\min[c_{44}(T, \nu)]$ and by $\max[\epsilon(T, \nu)]$ as freezing temperatures T_F^Q and T_F^D , respectively.

Figures 1 and 2 reveal that the dispersion regimes for strain and polarization are at different temperatures. For a quantitative comparison we plotted $\ln \nu$ vs $1/T_F^Q$ and $1/T_F^D$ for concentrations $x = 0.2$ and 0.5 (Fig. 3). The appearance of primary (α) and secondary (β) relaxation processes is a well-known phenomenon in polymers and glasses.²² In these systems the β relaxation exhibits an Arrhenius type of behavior, while the α relaxation often follows a Vogel-Fulcher law. Surprisingly, similar trends can be detected in Fig. 3.

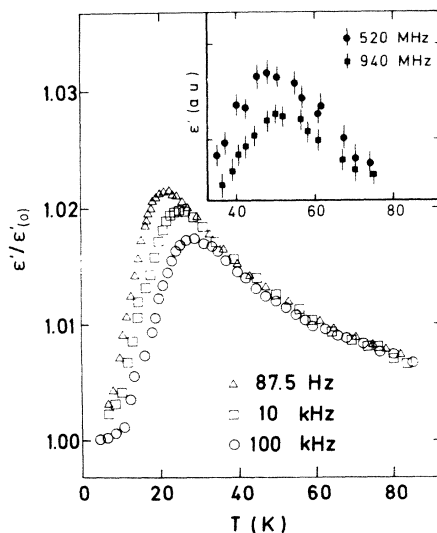


FIG. 2. Real part of the dielectric constant in $(\text{KBr})_{1-x}(\text{KCN})_x$ vs temperature for different measuring frequencies: 100 kHz (Ref. 11) (open circles); 10 kHz (Ref. 11) (open squares); 87.5 Hz (Ref. 11) (open triangles). Inset: the high-frequency data of this work; 520 MHz (full circles), 940 MHz (full squares).

$T_F^D(\nu)$ is well described by an Arrhenius law (broken line), while there seem to exist systematic deviations from the Arrhenius law in the quadrupolar relaxation. However, at present the very limited number of data points hamper a more quantitative analysis.

For both concentrations the freezing temperatures coincide only at gigahertz frequencies and high temperatures. At even higher temperatures the dynamics of quadrupoles and dipoles should be the same. However, as soon as the quadrupoles start to order, significant differences become apparent. In this sense the temperature where the rates meet could define the glass transition temperature T_G .²³ It is worthwhile to point out that gigahertz frequencies are close to the critical relaxation rate where all the alkali cyanides exhibit a transition from the plastic high-temperature phase into an orientationally ordered state.¹² At the glass transition temperature the onset of spontaneous random strains creates local distortions thereby increasing the barrier height and introducing an asymmetry into the reorientational potential.²⁴ Now the quadrupoles spend a longer fraction of time in a preferred orientation yielding a nonzero expectation value of the order parameter of the glass state.³

For the dielectric results we performed a rigorous

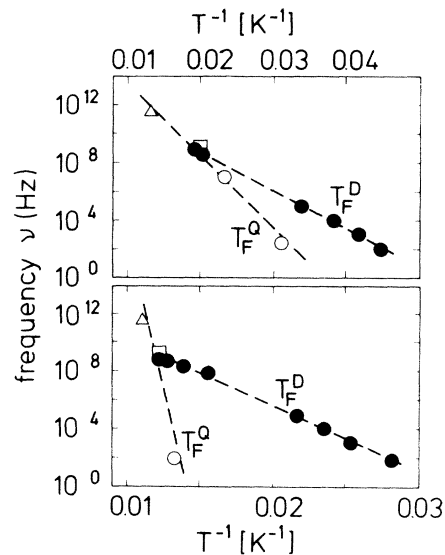


FIG. 3. Arrhenius plots ($\log \nu$ vs $1/T$) of the dipolar and quadrupolar freezing temperatures in $(\text{KBr})_{1-x}(\text{KCN})_x$ for concentrations $x = 0.2$ (top) and 0.5 (bottom). Full symbols represent dipolar data (this work and Ref. 11); open symbols denote quadrupolar data: inelastic-neutron-scattering studies (open triangles, $x = 0.2$, Ref. 9; $x = 0.5$, Refs. 4 and 5); Brillouin results (open squares, Ref. 20); ultrasonic results (open circles, Ref. 8); torsion pendulum measurements (open circles). The freezing temperatures are defined by the cusp maxima of the real part of the susceptibilities. The broken lines are the results of Arrhenius fits.

analysis fitting real and imaginary parts of the dielectric constant with an Arrhenius model including a distribution of relaxation times.¹³ This analysis yielded barrier heights $E_0 = 436$ K ($x = 0.2$) and 635 K ($x = 0.5$) and attempt frequencies $\nu_0 = 6.5 \times 10^{12}$ Hz ($x = 0.2$) and 2.9×10^{13} Hz ($x = 0.5$). In both samples the static dielectric susceptibility followed a Curie-Weiss law with Curie-Weiss temperatures $\theta = -11$ K ($x = 0.2$) and -50 K ($x = 0.5$) indicating paraelectric behavior of only weakly interacting dipoles even at 35 K.

For a direct comparison of quadrupolar and dipolar relaxation we have parametrized the cusp temperatures of the real parts of the susceptibilities in terms of the single-particle-potential Debye-Arrhenius model. The results, namely the hindering barrier E_0 and the attempt frequency $\tilde{\nu}_0$, are shown in Fig. 4. We are aware that the absolute values of E_0 and $\tilde{\nu}_0$ are overestimated (the hindering barriers by approximately a factor of 1.5, the attempt frequencies by three decades). But the general trends in the dipolar and the quadrupolar parameters are well established. Even allowing for these corrections, we find that reasonable quadrupolar barriers exist only for very low CN⁻ concentrations. With increasing x , E_0^Q and $\tilde{\nu}_0^Q$ increase and become unphysically large. In addition, it must be clearly stated that a description of relaxational phenomena in terms of an Arrhenius type of behavior describes the single-ion case only. Collective effects which we think drive

the quadrupolar freezing enter artificially into the free parameters yielding unrealistically high values of $\tilde{\nu}_0$ and E_0 . If one accepts these two parameters as a translation of collective effects into a single-ion picture, one should be aware that $\tilde{\nu}_0$ and E_0 can be rewritten in terms of alternative parameters E and ν_0 ,¹³ namely $\nu_0 = \tilde{\nu}_0 \exp(-\alpha/k_B)$ and $E = E_0 - \alpha T$. In this formulation the collective effects are cast more naturally into a linear temperature dependence of the hindering barrier. ν_0 is a real attempt frequency which could be visualized as the rotation frequency of the free CN rotator.

The high values and the strong concentration dependence of the quadrupolar single-ion Arrhenius parameters prove that the freezing in $(\text{KBr})_{1-x}(\text{KCN})_x$ is a cooperative phenomenon and that collective effects become more and more important as the concentration is increased. The contribution of the single-ion crystalline anisotropy to E_0 is of the order of 50 K and can be neglected for concentrations $x = 0.1$. A possible interpretation can be given in terms of a cluster formation process: At the glass transition the CN⁻ ions which are exposed to the strongest random strain fields are blocked in clusters leaving only cooperative relaxation channels for the molecular reorientation. The clusters grow with decreasing temperatures, thereby increasing the barrier height against molecular relaxation. The barrier heights against CN reorientations can now be visualized as the activation energy that is needed to move a domain wall across a cluster. A distribution of clusters gives the broad distribution of relaxation times that has been observed in $(\text{KBr})_{1-x}(\text{KCN})_x$.¹³

Conclusions concerning the origin of the dipolar hindering barriers are more difficult to draw. For all concentrations the dipolar freezing is measured in an orientationally ordered or in a quadrupolar glass state. Hence the Arrhenius parameters are relevant to a cubic crystalline potential with local deformations, only. Figure 4 suggests that the local environment is very similar in the quadrupolar glass and the quadrupolar long-range ordered state. There are no discontinuities at the critical concentration $x_c = 0.6$. Therefore we agree with Sethna, Nagel, and Ramakrishnan¹⁸ that the energy barriers to dipolar reorientations depend predominantly on the local deformation of the single-ion potential through quadrupolar interaction forces. However, at the moment there exist no experimental data that allow one to determine the importance of the dipolar interactions in the dipolar freezing process.

In conclusion, we have shown that the quadrupolar and the dipolar freezing in $(\text{KBr})_{1-x}(\text{KCN})_x$ are decoupled. The quadrupolar freezing is a cooperative phenomenon with strain-mediated interactions playing an important role, while the dipolar relaxation is a thermally activated process over the hindering barriers

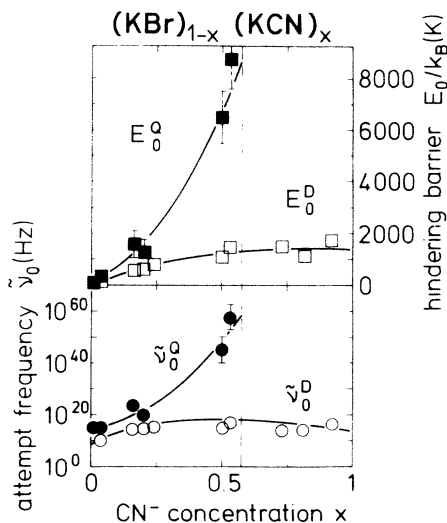


FIG. 4. Attempt frequencies $\tilde{\nu}$ and hindering barriers E_0 vs concentration x as derived from Arrhenius fits to the dipolar and quadrupolar freezing temperatures: dipolar parameters $\tilde{\nu}_0^D$ (open circles), E_0^D (open squares); quadrupolar parameters $\tilde{\nu}_0^Q$ (full circles), E_0^Q (full squares). The freezing temperatures have been determined from the real parts of the susceptibilities as described in the text.

created by the quadrupolar interaction energies.

We would like to thank J. M. Rowe for helpful discussions and M. Maglione for technical assistance. This work was partly supported by the Bundesministerium für Forschung und Technologie.

-
- ¹K. Knorr and A. Loidl, *Phys. Rev. B* **31**, 5387 (1985).
²J. M. Rowe, J. J. Rush, and S. Susman, *Phys. Rev. B* **28**, 3506 (1983).
³K. H. Michel and J. M. Rowe, *Phys. Rev. B* **22**, 1417 (1980).
⁴A. Loidl, M. Müllner, G. F. McIntyre, K. Knorr, and H. Jex, *Solid State Commun.* **54**, 367 (1985).
⁵J. M. Rowe, J. J. Rush, D. J. Hinks, and S. Susman, *Phys. Rev. Lett.* **43**, 1158 (1980).
⁶A. Loidl, R. Feile, and K. Knorr, *Phys. Rev. Lett.* **48**, 1263 (1982).
⁷C. W. Garland, J. Z. Kwiecien, and J. C. Damien, *Phys. Rev. B* **25**, 5818 (1982).
⁸R. Feile, A. Loidl, and K. Knorr, *Phys. Rev. B* **26**, 6875 (1982).
⁹A. Loidl, K. Knorr, R. Feile, and J. K. Kjems, *Phys. Rev. Lett.* **51**, 1054 (1983); A. Loidl, R. Feile, K. Knorr, and J. K. Kjems, *Phys. Rev. B* **29**, 6052 (1984).
¹⁰S. Bhattacharya, S. R. Nagel, C. Fleishman, and S. Sus-

man, *Phys. Rev. Lett.* **48**, 1267 (1982).

- ¹¹K. Knorr and A. Loidl, *Z. Phys. B* **46**, 219 (1982).
¹²F. Lüty and J. Ortiz-Lopez, *Phys. Rev. Lett.* **50**, 1289 (1983).
¹³N. O. Birge, Y. H. Jeong, S. R. Nagel, S. Bhattacharya, and S. Susman, *Phys. Rev. B* **30**, 2306 (1984).
¹⁴J. J. De Yoreo, M. Meissner, R. O. Pohl, J. M. Rowe, J. J. Rush, and S. Susman, *Phys. Rev. Lett.* **51**, 1050 (1983).
¹⁵D. Moy, J. N. Dobbs, and A. C. Anderson, *Phys. Rev. B* **29**, 2160 (1984).
¹⁶B. Fischer and M. W. Klein, *Phys. Rev. Lett.* **37**, 756 (1976), and **43**, 289 (1979).
¹⁷J. Ihm, *Phys. Rev. B* **31**, 1674 (1985).
¹⁸J. P. Sethna, S. R. Nagel, and T. V. Ramakrishnan, *Phys. Rev. Lett.* **53**, 2489 (1984).
¹⁹G. Pakulski, *J. Phys. E* **15**, 951 (1982).
²⁰S. K. Satija and C. H. Wang, *Solid State Commun.* **28**, 617 (1978).
²¹In the ultrasonic experiments the signals are lost because of heavy damping (Refs. 7 and 8); in the inelastic-neutron-scattering experiments the loss is hidden in the temperature-dependent broadening of the phonon linewidth. An analysis of the neutron data is model dependent and limited by the experimental resolution.
²²G. P. Johari, *Philos. Mag. B* **46**, 549 (1982).
²³J. M. Rowe, private communication.
²⁴H. T. Stokes and R. D. Swinney, *Phys. Rev. B* **31**, 7133 (1985).